Biosensors and Bioelectronics 146 (2019) 111746

Contents lists available at ScienceDirect

Biosensors and Bioelectronics

journal homepage: http://www.elsevier.com/locate/bios

# Separation detection of different circulating tumor cells in the blood using an electrochemical microfluidic channel modified with a lipid-bonded conducting polymer

N.G. Gurudatt [a,d], Saeromi Chung [a], Jung-Min Kim [a], Moo-Hyun Kim [b], Dong-Keun Jung [c], Jin-Young Han [c], Yoon-Bo Shim [a,*]

[a] Department of Chemistry and Institute of BioPhysio Sensor Technology, Pusan National University, Busan, 46241, Republic of Korea
[b] Department of Cardiology, Dong-A University College of Medicine, Busan, 602-715, Republic of Korea
[c] Department of Laboratory Medicine, Dong-A University College of Medicine, Busan, 602-715, Republic of Korea
[d] National Efficacy Evaluation Center for Metabolic Disease Therapeutics, Lee Gil Ya Cancer and Diabetes Institute, Gil Medical Center, Gachon University, Incheon, 21565, Republic of Korea

ARTICLE INFO

*Keywords:*
Circulating tumor cells
Cancer detection
Conducting polymer
Amperometric separation detection
Electrochemical microfluidic device

ABSTRACT

Different circulating tumor cells (CTCs) in blood were separated and detected through the decoration of anti-cancer drug on the target cells, along with chemical modification of the microfluidic channel walls using a lipid attached covalently to the conducting polymer. The working principle of the electrochemical microfluidic device was evaluated with experimental parameters affecting on the separation, in terms of mass and surface charge of target species, fluid flow rate, AC amplitude, and AC frequency. The separated CTCs were selectively detected via the oxidation of daunomycin adsorbed specifically at the cells using an electrochemical sensor installed at the channel end. The fluorescence microscopic examination also confirmed the separation of CTCs in the channel. To evaluate the reliability of the method, blood samples from 37 cancer patients were tested. The device was able to separate the CTCs with 92.0 ± 0.5 % efficiency and 90.9% detection rate.

## 1. Introduction

The spread of cancer in the body is attributed to the metastasis of tumor cells from their location of origin to the different organs in the body (Mehlen and Puisieux, 2006). To successfully cure cancer, it is necessary to detect the presence of these cells before they metastasize and form secondary tumors, eventually causing cancer (Etzioni et al., 2003). During the early stages of metastasis, the circulating tumor cells (CTCs) from a primary tumor travel through the bloodstream (Ashworth, 1868). They are rare, and account for as low as one cell per $10^9$ hematologic cells in the blood of metastatic cancer patients; and the CTCs are very similar in size as compared to some of the WBCs, hence, their separation is a tremendous challenge (Rolle et al., 2006; Zieglschmid et al., 2005; Kahn et al., 2004; Krivacic et al., 2004; Nagrath et al., 2007).

Conventionally, the identification of CTCs has been done by microscopic examination of the blood samples collected from the patients (Eunice et al., 2013), however, a more advanced approach is the integration of microfluidic technology with biochemical analysis (Karabacak et al., 2014; Zhang and Nagrath, 2013; Bleilevens et al., 2018; Tang et al., 2019). Previously, the CTCs separation has been effectively carried out using metallic/magnetic beads decorated on the cancer cells (Jiang et al., 2015) for the clinical use in transfusion medicine for treating hematological disorders, where the separation of the leukocytes labelled with magnetic beads has performed at a preparatory level (Lenshof and Laurell, 2009). However, magnetic bead-based technologies are prone to a certain level of biological noise, which can contribute to their low sensitivity, prohibiting their capacity for selective early detection of cancer in human fluid samples (Nagrath et al., 2007). Hence, strategies have been developed recently to incorporate the identification of surface bound antigens to aid in a microfluidic separation (Phillips et al., 2009). These cell separation methods involve the attachment of antibody tags to specific cell types in a mixed solution (Nagrath et al., 2007; Desitter et al., 2011; Adams et al., 2008). However, to perform this, one must have preliminary knowledge regarding the type of cancer. Some of the recent works have ventured to separate

* Corresponding author.
*E-mail address:* ybshim@pusan.ac.kr (Y.-B. Shim).

https://doi.org/10.1016/j.bios.2019.111746
Received 25 September 2019; Accepted 28 September 2019
Available online 30 September 2019

the CTCs based on their physical properties using dielectrophoresis, flow fractionation, acoustics, and cell enrichment by specialized microstructures in the channel etc. (Moon et al., 2011; Li et al., 2015) While these methods achieved high efficiency, they could only separate one type of cancer cell from the diluted blood samples. To date, CellSearch® is the only FDA approved method for sorting CTCs from blood samples. Using this method, only CTCs of epithelial origin can be separated.

Thus, a new robust method is needed to separate and analyze the CTCs for the early-stage diagnosis of cancers. To overcome the disadvantages of the conventional microfluidic cell separation system and to achieve a size dependent separation of CTCs with high efficiency, we have devised a new electrochemical microfluidic channel, structured with screen-printed carbon electrode walls. Where, it is observed that the uniform and symmetrical AC electric field have been applied to the channel walls for the complete CTCs separation. In addition, since the cancer cell surfaces show an altered expression of glycoconjugates (glycoproteins and glycolipids), with an increased expression of sialic acid, heparin sulfate, anionic lipids, and other anionic molecules, which are more negative in nature compared to normal cells (Sanders et al., 1989; Varki et al., 2009). Thus, the cancer cells, preferably participate to interface with the positively charged lipid-modified surfaces to a large extent through lipid-lipid and charge interactions (Gurudatt et al., 2016). This modification expected to give more effective partition of cancer cells along with AC field perturbation in the channel, resulting in the precise separation and enrichment of the CTCs.

In the present study, a stable lipid-bonded polyterthiophene layer formed on the channel walls provided a unique surface characteristic for the interaction with cancer cells. At first, the amine functionalized conducting polymer precursor, [2,2':5′,2″-terthiophene]-3′,4′-diamine (DAT) was electrochemically polymerized onto the channel walls to act as a substrate material to support the immobilization of the lipid molecules (phosphatidylserine) (Kwon et al., 2006; Rahman et al., 2003). After separation, to detect the electrochemically inactive CTCs, the tetracycline compound daunomycin (DM) has been selectively interacted with the cancer cell surface prior to the separation experiment, the same procedure was also followed for the blood samples (Chandra et al., 2013). The primary criterion for CTCs separation was the difference in cell size (mass) and surface charge, however, it was coupled with the altered chemical state on the cell surface. The separated CTCs, which are depending on their movement inside the channel because of their size variation, were detected amperometrically at the carbon electrode installed at the channel end. The reliability of the method was evaluated with blood samples from cancer patients.

## 2. Experimental section

### 2.1. Chemicals and apparatus

All the chemicals used in the study were of extra pure quality obtained from Sigma Aldrich and used as received. All the electrochemical experiments were conducted in a three-electrode system using a Kosentech PT-1 potentiostat/galvanostat (S. Korea). The microfluidic channel was fabricated using Bando Industrial Model BS- 450HT (South Korea) screen printing machine. The surface characterization of the channel walls modification was done using XPS and FE-SEM at Korea Basic Science Institute (KBSI). QCM was performed using a SEIKO EG & G model QCA 917 and a PAR Model 263A potentiostat/galvanostat. A gold coated working electrode (area: 0.196 $cm^2$; 9 MHz; AT-cut quartz crystal) was used for the QCM experiment. A function generator (GSI-Model Protek 9340, South Korea) was used for supplying the AC electric field on the wall electrodes. For injecting sample into the microchannel, a miniaturized automated microsyringe pump (Twins syringe pump Model-33, Harvard Apparatus, USA) was used. A diamine functionalized terthiophene monomer, [2,2':5′,2″-terthiophene]-3′,4′-diamine (DAT) was synthesized according to the previously reported procedure (Rahman et al., 2003). Cervical cancer HeLa, lung Cancer A549, breast adenocarcinoma MDA-MB-231, normal breast MCF-10A, and acute T cell leukemia Jurkat clone E6-1 cell lines were obtained from the Korean Cell Line Bank (South Korea). Dulbecco's Modified Eagles Medium (DMEM), Roswell-Park Memorial Institute (RPMI)-1640 medium, Penicillin/Streptomycin, Fetal Bovine Serum (FBS), Horse serum, Trypsin-EDTA, Dulbecco's phosphate buffered saline (for cell culture), Propidium iodide (PI), fluorescein diacetate (FDA), 1-ethyl-3-[3-(dimethylamino) propyl]-carbodiimide (EDC), N-hydroxysuccinimide (NHS), retinoic acid, phosphatidyl choline (PC), epidermal growth factor, folic acid, folinic acid, pemetrexed, methotrexate, and raltitrexed were obtained from Sigma Aldrich. Tetrabutyl ammonium perchlorate (TBAP; electrochemical grade) was obtained from Fluka Co. and dried in a vacuum. Phosphate-buffered saline (for electrochemical measurements) was prepared with 0.01 M disodium hydrogen phosphate, and 0.01 M sodium dihydrogen phosphate (Aldrich). All other chemicals were of extra pure analytical grade and used without further purification. Deionized water (18 MΩ cm) from a Direct-Q system (Millipore, Billerica, MA) was used to prepare all aqueous solutions. The blood sample flow in the microfluidic channel was observed through an optical microscope (Olympus BX51; Olympus Co., Ltd., Tokyo, Japan) with a 10× objective lens. The flow in the microfluidic device was consecutively captured by a high-speed camera (Phantom VEO710L, Vision Research Inc., Wayne, NJ, USA) at 200 fps (frame per second) (Yeom et al., 2014).

### 2.2. Fabrication of microfluidic channel

The electrochemical microfluidic channel (EMFC) was prepared by screen printing the carbon ink on a glass slide, the thickness of the channel was maintained to obtain the adequate width (95.0 ± 2.5 μm) and height (15.0 μm) of the channel (Fig. S1) (Noh et al., 2012). The printed channel was dried for 2 day at 60 °C. Each area of working, reference, and counter electrodes and channel walls obtained by screen printing were checked for their connectivity to see that they are not connected to one another and properly separated. Then, the channel was covered by a second glass slide, leaving the electrode connector areas open for access. This channel device was tested for free flow of liquid by flowing distilled water through it for prolonged periods. The channel was then cased with a homemade connector module which facilitated the easy electrical connections to the channel, this was further covered with a secondary cover using a strong epoxy, which acts as a faradaic cage and allows for noise reduction during data acquisition/analysis. The channel wall was modified with a layer of functionalized polyterthiophene as a supporting material for the immobilization of lipid layer. To form the polymer layer on the channel wall, the DAT monomer was dissolved in a mixture of acetonitrile and water to form 1.0 mM solution containing 0.1 M TBAP as supporting electrolyte, the monomer solution was then filled in the microfluidic channel and the potential cycling was carried out on both the channel walls from 0 to 1.4 V for two cycles. The polymer layer formed on the walls was used as an anchor to covalently attach lipid molecules on the channel walls. The lipid was incubated with 10 mM each of EDC and NHS in a 0.1 M PBS to activate the carboxylic acid group of lipids. This solution was then filled in the channel and allowed to react for 6 h. Due to the activation of carboxylic acid groups (-COOH) of the lipid molecules by the carbodiimide, the amine functional groups (-$NH_2$) of the polymer layer form strong bonds with the lipid molecules to give a stable lipid modified surface on the channel walls.

The electrochemical microfluidic channel was connected to an AC function generator and a potentiostat. The channel walls on both sides were connected to an AC function generator to apply and modulate the AC field (frequency and amplitude) to facilitate the separation process. The leads from the detection electrodes at the channel end are connected to a potentiostat. Known concentrations of the cultured cells were interacted with 0.1 μM DM for 30 min in PBS at 4 °C and loaded into the channel after washing.

### 2.3. Cell culture

HEK-293, and HeLa (KCLB) were cultured in T75 culture flask in a Dulbecco's modified eagle's medium supplemented with 10% FBS and 1% penicillin-streptomycin in a CO2 incubator at 37 °C. Jurkat E6-1 clone cells were cultured in RPMI-1640 medium supplemented with 10% FBS and 1 % penicillin-streptomycin as a suspension culture. The culture media were changed once in every two days until 95% confidence was obtained. The cells were removed from culture by trypsinization followed by three times washing in Dulbecco's PBS to remove any remaining media and serum. The cells thus obtained were re-suspended in a known volume of PBS to obtain a known concentration of cells. The cell suspension was allowed to settle for 5 min in the CO2 environment to get the cells in the most possible healthy condition.

### 2.4. Preparation of blood sample

Patient blood samples were freshly obtained from Dong-A University Hospital. 1 ml of the whole blood was incubated with 0.1 μM of daunomycin (DM) at 4 °C to avoid internalizing of the drug into the cells. After 30 min of incubation the blood sample was centrifuged at 1000 rpm for 5 min at 4 °C to separate any un-interacted/free DM along with the plasma content leaving behind only the cellular content of the blood as the pellet. This pellet was washed three times with physiological saline (0.9 % NaCl) and re-suspended in PBS to get a diluted suspension of blood cells. The above obtained solution was loaded in the microfluidic channel for the analysis.

### 2.5. Electrochemical microfluidic setup for the separation and detection of CTCs

The leads from the cover are connected to a potentiostat as working, reference, and counter electrodes which are present at the end of the channel. The channel walls on both sides were connected to a function generator to apply and AC frequency and amplitude to facilitate the separation process. Before starting the experiment, the channel was made sure of allowing a free flow of liquids by running buffer through it. The applied potential for the detection of DM molecules present on the CTCs was set at −0.75 V as the molecule was oxidized at −0.7 V. The blood sample was then run through the channel at a flow rate of 5 μL/min for 5 min making it over all 25 μL of the sample in the pre-channel piping. By this time the sample reached the reservoir at the start of the channel. When the buffer is running at a flow rate of 2.5 μL/min, the slow flow rate is maintained to allow the separation of the cells inside the channel and to allow the cancer cells to interact with the lipid molecules present on the channel wall. A double step chronoamperometry is simultaneously started with the buffer flow to observe the changes at the detection zone.

## 3. Results and discussion

### 3.1. Separation principle of the EMFC

The EMFC was constructed as shown in Scheme 1. Where, the electrical field in high frequency was applied to the channel walls for separation, symmetrically. In this case, the movement of cells along y-axis in the channel during the application of the electric field can be derived from the Newton's second law of motion. When we apply the AC field (A, ω, and d) on the channel walls without the hydrodynamic flow of the medium along x-axis, the position and velocity of target species in the channel are changed along y-axis as the function of mass and charge. The AC electrical force exerted to the target species causes them to accelerate away from or to each channel wall; the force in the opposite direction applied to the species from the other channel wall makes them to have an oscillation between the channel walls. Eq. (1) demonstrates the oscillation induction in the target species (y-axis) in the channel, which is pivotal in the mass dependent separation of the target species. Hence, the motion of the target species suspended in a Newtonian fluid because of the electric field application is governed by Eq. (1).

$$y(t) = -\frac{qE_0(\cos \omega t - 1)}{6\pi\eta Rw} + y_0 \quad (1)$$

where, $y(t)$ is the position of the particle with radius R at the given time t, q is the charge on the target species. The term ω is given by 2πf, where $f$ is the applied AC frequency and $E_0$ is the amplitude of the electric field. R is the radius of the particles, $\eta$ is the viscosity coefficient of the medium and $y_0$ is the initial position of the particle. The computer simulation of this equation can be confirmed using Fig. S10.

Since the channel wall is symmetrically configured, the induced velocity of the medium is negligible, therefore, we can assume the media motion as constant. From Eq. (1), we can demonstrate that the target movement from initial position in the electric field according to time. The position of target species in the flow and their distance from the walls greatly influenced by the strength of the electric field applied. In this condition, when the hydrodynamic flow is introduced, the Newtonian movement follows the Navier-Stokes equation (Etienne et al., 2001; Colin, 2004). The target species move with a combination of y-axis motion and the hydrodynamic flow along the x-axis direction causing a wavelike motion.

The different physical property and chemical composition of the

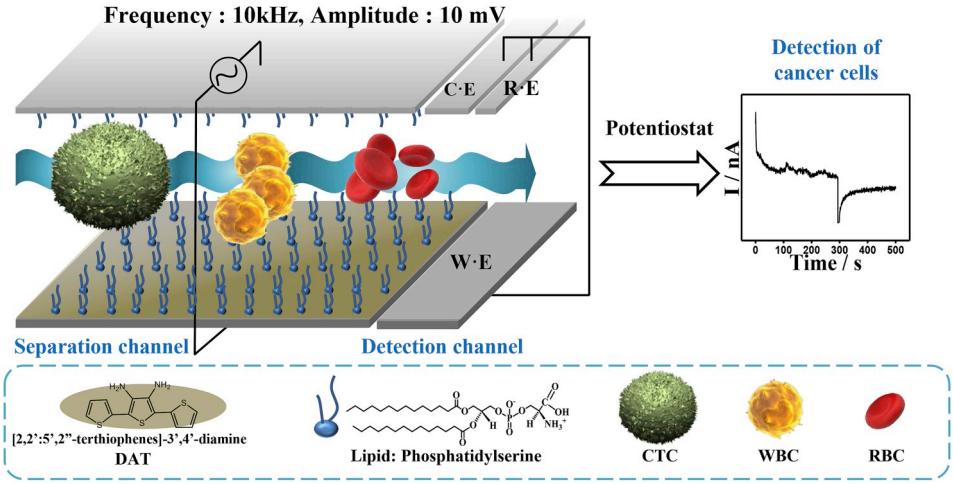


**Scheme 1.** The schematic representation of the design and fabrication of the proposed microfluidic channel.

CTCs can make the separation of them, precisely. The cells with small size will have faster movement and therefore shorter elution time, whereas the large cells will have low velocity, hence, longer retention time. Using this criterion, cells in the different chemical composition and sizes can be effectively separated using the proposed device. Optimizing the parameters affecting the AC electric field strength (frequency and amplitude), the separation of different kinds of CTCs can be achieved as shown in Fig. 2. The strength of the electric field exposed to separation medium was determined by simulating an equivalent circuit for the channel configuration. The overall electric field applied to the medium was calculated to be 0.0008 kV/cm at a capacitance of 0.5 μF and a frequency of 10 kHz (optimal for CTC separation). Researchers had studied for the separation enumeration of tumor cells and their apoptosis by optofluidic system (Guo et al., 2015a,b, 2015a,b). Their detection accuracy was depended on the position of the cells during the movement in the hydrodynamic flow. In these cases, hydrodynamic sheath flow was observed as the driving force. However, in our case, inertial movements of electroosmotic slip flow and electrophoretic flow were the driving forces of the cell displacement in the AC field applied-microfluidic channel.

### 3.2. Characterization of modified microfluidic channel

To fabricate the EMFC, the carbon-printed channel device was dried and covered with a glass cover to form a free-flowing channel with the inbuilt electrochemical three electrode system (Fig. S1). The channel was printed with a depth of 15.0 ± 1.5 μm to give specific volume in the channel. The bare carbon channel shows little/no separation between

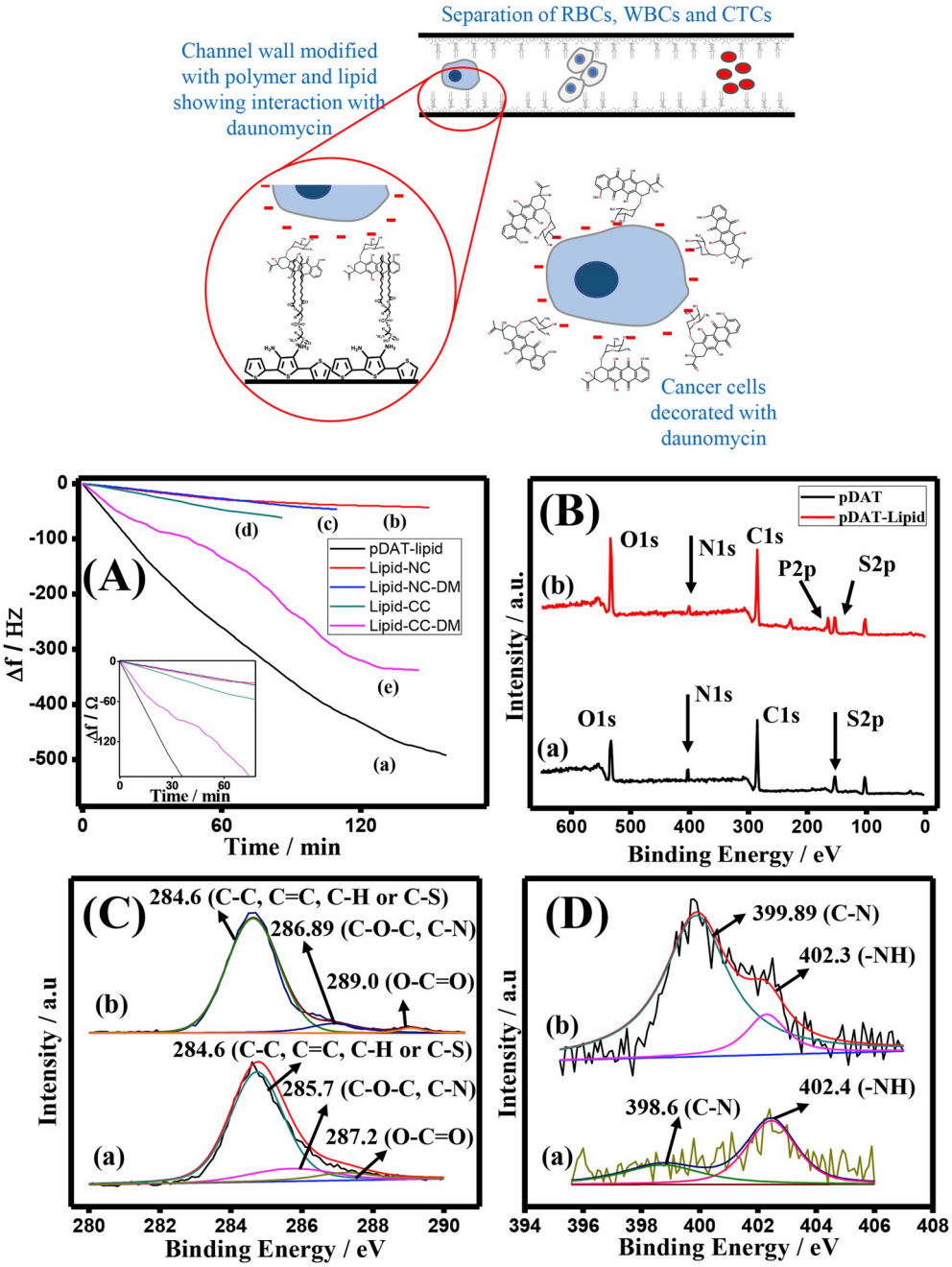


**Fig. 1.** (A) Frequency changes obtained from QCM analysis for (a) the immobilization of lipids on the pDAT surface, (b) normal cells without DM, (c) normal cells with DM, (d) cancer cells without DM, and (e) cancer cells with DM. (B) XPS survey spectra of the channel wall modification. (C) and (D) Deconvoluted C1s and N1s spectra of (a) pDAT and (b) pDAT-lipid modified surfaces, respectively.

different cancer cells. Hence, the channel walls were modified to achieve a slight interaction with the CTCs to considerably slow them in the channel as compared to the other hematopoietic cells. The electropolymerization of the DAT monomer was carried out using the potential cycling method in acetonitrile/water (1:1) solution (Fig. S2 (A)). Two oxidation peaks were observed at 0.76 and 1.53 V respectively, confirming the formation of the polymer layer on the walls (data not shown), followed by the immobilization of the lipid layer (Fig. S2 (B)). The channel wall modified with lipid layer (phosphatidylserine) was characterized by impedance spectrometry. Impedance spectra (from 100 kHz to 100 mHz at 100 mV) obtained for the modified channel walls in 0.1M PBS show that the charge transfer resistance increases after the electrochemical polymerization of DAT on the bare channel wall from 16.7 kΩ to 25.4 kΩ, suggesting the successful formation of the polymer layer (Fig. S3 (a and b)). A further increase in the resistance to 37.5 kΩ from 16.7 kΩ was observed after lipid immobilization (Fig. S3 (c)), confirming the successful bound of lipid molecules.

To further confirm the electro-polymerization and the immobilization of the lipid layer, the XPS analysis was performed. Both polymer and polymer-lipid layers show the characteristic XPS peaks for carbon, nitrogen, and oxygen atoms. As shown in Fig. 1B (a), obtained for the DAT polymer (pDAT) layer, C1s, N1s, and S2p peaks (284.7 eV, 402.9 eV, and 164.66 eV) confirming the presence of the terthiophene backbone and amine groups. The small O1s peak at 532.8 eV is due to the surface impurity. After the chemical immobilization of the lipid through the amide bond formation, the pDAT-lipid layer shows all the expected peaks observed previously for the pDAT surface and an additional new P2p peak is observed at 163.9 eV, which corresponds to the P atom present in the lipid molecule that confirms the successful bind of the lipid on the polymer surface as shown in Fig. 1B (b). The deconvoluted C1s spectra shows three distinct peaks for the pDAT modified layer (Fig. 1C (a)), where the peak at 284.6 eV represents the presence of C–C, C–H, and/or C–S bonds which also show the presence of sulfur atom in the polymer layer. The peak at 285.7 eV corresponds to the C–N bond confirming the presence of nitrogen (-$NH_2$) in the polymer. This peak shifted to 286.89 eV after the immobilization of the lipid, indicating the change in the configuration of the C–N bond, which in turn confirms the formation of the amide bond between the polymer and the lipid (Fig. 1C (b)). The N1s spectra for the pDAT modified surface show two ideal peaks at 398.6 eV and 402.4 eV corresponding to C–N and –N-H bonds, respectively as shown in Fig. 1D (a). When the lipid molecule was immobilized on the polymer surface through the EDC/NHS treatment, the C–N peak has shifted 1.29 eV from 398.6 eV to 399.89 eV along with an increase in its intensity (Fig. 1D (b)). This indicates the change in the electronic states of nitrogen atoms by the formation of amide bond and the increase in the composition of C–N bonds and proving the successful immobilization of the lipid molecules on the channel wall.

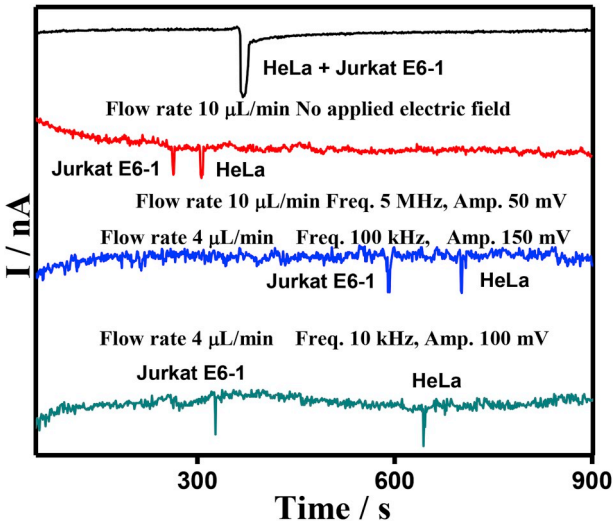


**Fig. 2.** Chronoamperograms for the optimization of flow rate, frequency, and amplitude for the successful separation of different cancer cells (HeLa and Jurkat E6-1).

### 3.3. Monitoring of cell-daunomycin interaction

To confirm the specificity of the interaction between DM and cancer cells, cultured cells (HeLa and HEK-293) were incubated with 0.1 µM DM solution at 4 °C for 35 min. These cells were washed three times with DPBS, and the free DM was removed; the DM treated cells were then re-suspended in DPBS to get a known cell concentration. The samples of normal and cancer cells were drop casted on glassy carbon electrodes separately, and the CVs were recorded between −0.2 and −0.8 V at a scan rate of 50 mV/s in deoxygenated PBS. The voltammograms reveal that the DM treated non-cancerous (HEK-293) cells show little or no electrochemical response to the DM molecules (Fig. S4 (a)). However, the similarly treated cancerous (HeLa) cells show a prominent redox couple at −0.6/-0.65 V, indicating the successful adsorption of DM onto the cancer cells as shown in Fig. S4 (b). The absence of a response in the case of normal cells indicates the lack of interaction between the DM and the cell surfaces. The lack of interaction might be due to unaltered surface glycolipids and glycoproteins, the surface charge of the cells or both.

### 3.4. Detection of CTCs using EMC

To detect the CTCs, we monitored the redox peak of the DM adsorbed on the cells. The blank PBS solution showed no response (Fig. 3 A (a)), whereas the DM-treated cancer cells in PBS showed a distinct peak due to the oxidation of DM molecules adsorbed, as shown in Fig. 3 A (b), confirming the presence of CTCs in the microfluidic channel. Different numbers of cells ($1 \times 10^2$, $1 \times 10^3$, $1 \times 10^4$, $1 \times 10^5$, and $2.5 \times 10^5$ cells/mL) were spiked into a healthy human whole blood sample and treated with DM and processed as before. As the number of spiked cancer cells ($1 \times 10^2$, $1 \times 10^3$, $1 \times 10^4$, $1 \times 10^5$, and $2.5 \times 10^5$ cells/mL) increased, the peak area also increased, indicating that the magnitude of response signal was dependent on the number of cancer cells and not on the size of the cancer cells (Fig. 3 B). The calibration curve was plotted for the concentration of cells against the response current (Fig. 3 C). The efficiency of the method was evaluated by determining the lowest number of detectable cells per mL of blood. A single cell was successfully separated and detected by this device (7 cells/mL) as shown in Fig. 3 D. To measure the retention time of the cells without DM-treatment, 0.1 µM DM solution was loaded in the microfluidic channel as a sample and was separated to confirm the response of the molecules in the channel. An oxidation peak isolated in the chronoamperograms at 37s indicated the localization and separation of DM molecules in the channel (inset of Fig. 3 D).

The electrochemical signal obtained was considered an indicator for the collection of cells at the end of the channel. The number of cells recovered from spiked ones ($1 \times 10^2$, $1 \times 10^3$, and $1 \times 10^4$ cells/mL) in the blood sample (Fig. S5 A, B, and C). Finally, the collection efficiencies were plotted against the number of cells as shown in Fig. S6 (A). The electrochemical microfluidic device was able to separate up to an average of $95 \pm 1.5$ % of the spiked cancer cells with $92 \pm 0.5$ % efficiency, avoiding the RBCs and WBCs. The results from a series of experiments for the recovery of both WBCs and CTCs are shown in Fig. S6 (B).

### 3.5. Real sample analysis

The blood samples from patients with different cancers were collected and treated with the DM. The samples were from varied sex and age groups at different stages as listed in Table 1. 20 of 22 samples

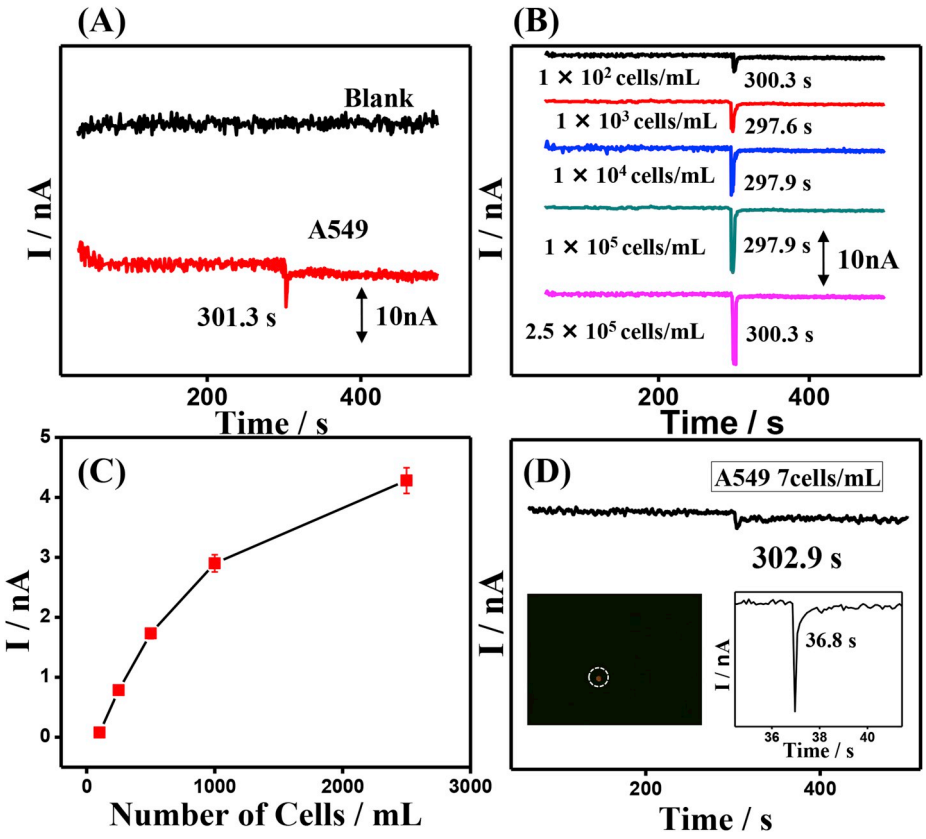


**Fig. 3.** (A) Chronoamperograms for the (a) blank and (b) A549-spiked PBS samples. (B) Amperometric responses of blood samples spiked with different amount of cancer cells ($1 \times 10^2$, $1 \times 10^3$, $1 \times 10^4$, $1 \times 10^5$, and $2.5 \times 10^5$ cells/mL). (C) Calibration plot for spiked cancer cells. (D) Separation of the lowest number of cancer cells (7 cells/mL) in the channel; inset of (D) fluorescent image of a single cell separately collected from the channel, and control detection of free DM.

**Table 1**
Tabulation of the patient blood samples analytically detected, and the actual results provided by the hospital.

| Sample | Age (Yrs) | Sex | Type of cancer | Stage of cancer | Size of cancer (cm) | Marrow blasts (%) | Detection | No. of cells/ 100 μL | Remarks |
|---|---|---|---|---|---|---|---|---|---|
| 1 | 71 | M | Stomach cancer | T2N1, stage IIA | 2.5 × 1.7 | | | 8 | |
| 2 | 60 | F | Breast cancer | T4N3M1, stage IV | | | | 7-8 | Multiple metastasis |
| 3 | 73 | F | Pancreatic body cancer | TXNXM1, stage IV | 3 | | | 5 | Liver metastasis |
| 4 | 60 | F | Breast cancer | T1N1M1 | 1 × 0.8 | | | 3 | |
| 5 | 57 | F | Breast cancer | T1N0M0, stage IA | 5 | | | 6 | |
| 6 | 58 | F | Breast cancer | T4N3M0, stage IIIB | 10 × 9 | | | 6 | Lymph metastasis |
| 7 | 73 | M | Lung cancer (adenocarcinoma) | T2bN1M0, stage IIB | 6 × 5.1 | | | 7 | Lymph metastasis |
| 8 | 66 | F | Stomach cancer | | 2 | | | 5 | |
| 9 | 49 | F | Breast cancer | T1N0 | | | | 3 | |
| 10 | 38 | M | Stomach cancer | | | | | 3 | EGC |
| 11 | 36 | F | Skin of scalp & neck cancer | | | | X | 0 | SCC |
| 12 | 70 | F | Bladder cancer | stage T1 | 2.3 | | | 1 | |
| 13 | 60 | F | Nasopharyngeal cancer | T3N2Mx, stage III | | | | 5 | Lymph metastasis |
| 14 | 59 | F | Non-small cell lung cancer | T2N3M1b, stage IV | 1.9 × 1.9 x 1.9 | | | 4 | Multiple metastasis |
| 15 | 57 | M | Esophageal cancer | | | | X | 0 | Multiple metastasis, SCC |
| 16 | 42 | F | Ampulla of Vater cancer | TxNxM1, stage IV | 2.5 × 2.5 | | | 3 | Multiple metastasis |
| 17 | 48 | M | T-ALL | | | 92.8 | | 7 | Hematologic malignancy |
| 18 | 74 | F | Colon cancer | TxNxM1, stage IV | | | | 8 | Liver metastasis |
| 19 | 72 | F | Pancreatic cancer | TxNxM1, stage IV | | | | 4 | |
| 20 | 58 | F | Breast cancer | TxNxM1, stage IV | 3.5 × 3.1 x 3.8 | | | 6 | Lymph metastasis |
| 21 | 68 | M | B-ALL | | | 87.8 | | 8 | Hematologic malignancy |
| 22 | 61 | F | Rectal cancer | TxNxM1, stage IV | 3.8 × 3.5 | | | 5 | Multiple metastasis |

were successfully separated in the microfluidic channel, then the CTCs were collected. The number of cancer cells collected varies from in repeated experiments, indicating an uneven distribution of CTCs in the blood samples. Sample No. 11, squamous cell carcinoma and sample No.15, esophageal (squamosal) cancer with multiple metastasis were undetected. Since both the undetected samples share a common origin of squamosal cells, it might be related to the non-detectable cell environment. Hence, these samples have been considered as errors and the method showed a 90.90% detection rate.

Furthermore, to evaluate the reliability of the method, 15 new patient samples were collected and blind tested using the proposed method. 9 of 15 samples showed the electrochemical response based on the DM oxidation at different retention times, indicating the presence of different kinds of cancer cells. The results obtained were then matched with the information obtained from the hospital and were tabulated in Table S1. The chronoamperograms in Fig. 4 show separation peaks at a different retention time for different samples, which agree with the corresponding theoretical and practical size of the cancer cells. Sample No. 33, breast cancer shows metastasis into the liver and bone and was detected at a retention time of 391.3 s (Fig. 4A (a)) and sample No. 36, acute lymphocytic leukemia was detected at 186.3 s (Fig. 4A (c)), whereas sample 25 and 35, acute myeloid leukemia both from two different patients of the same sex and age group, were detected at the same retention time of 202.5 s (Fig. 4A (b and d)) indicating a proper separation of CTCs.

The samples from healthy persons showed no response during separation along with some of the cancer patient samples, which have not yet metastasized. Sample No. 27 (Osteosarcoma) and 32 (Non-small cell lung cancer) have considerable tumor size (4 cm) but have not metastasized, hence we did not observe any response; and sample 23 (blood cancer) (21 %) also did not show a positive response. After the separation, the cells were collected using a micro-syringe and observed under a fluorescent microscope; due to the inherent fluorescent properties of the DM molecule present on the cancer cells, the separated cells were clearly seen at 590 nm (Fig. 4 (B) (a-d)). The images of the collected sample show that detection of even a single cell is also possible using the proposed method.

To evaluate the device capability to differentiate and separate CTCs of different origin and size, we have combined six different cultured cancer cells and separated them from one another using the proposed system. The cell samples belonging to stomach, B-cell acute lymphoblastic leukemia, lung (adenocarcinoma), non-small lung cancer, T-cell acute lymphoblastic leukemia, and breast cancers were chosen due to the difference in their size and the places of origin which determines the extent of the surface alterations (expression). Because of these, the cells have different interactions with the modified channel surface. To separate all the six different cancer samples, the flow rate had to be optimized to 5.0 μL/min. When the electric field with an optimized flow rate is applied, the cells move towards and away from the channel wall to give a wavelike motion interacting with the channel wall. This brings the same sized cells together, making them to separate from the other cells. As shown in Figs. 4C and 6 different separation peaks were observed at different retention times. To assign the peaks to a particular type of cancer, we have run the cell samples individually in the microchannel and the corresponding retention times were noted as shown in Fig. 4D. All the samples showed agreeable retention times as compared to the mixed separations, showing the applicability of the proposed microchannel system to separate real samples. In order to achieve the separation of same sized cells of different origin, we have to include a different criterion for the interaction of CTCs with the separation channel. The collected cells were also tested for viability by trying to grow them in culture, however, the cells were not viable since the cells were treated with a potent anticancer drug, daunomycin. To confirm the lack cell membrane damage by the applied electric field, we have

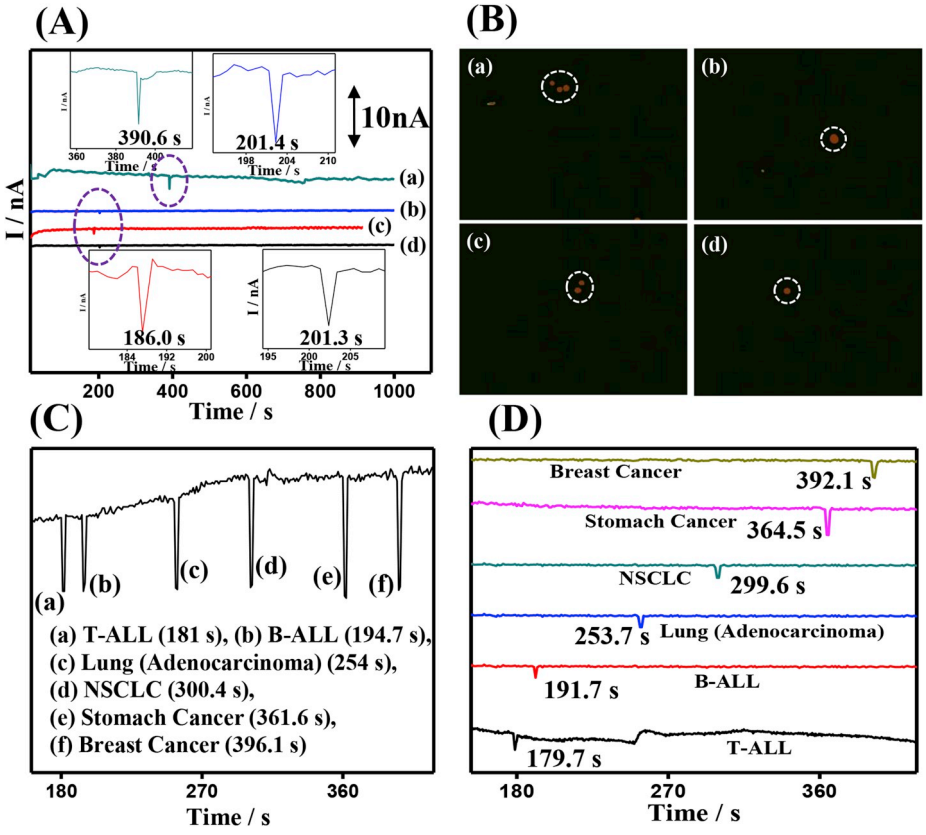


**Fig. 4.** (A) Chronoamperograms for the separation of CTCs from the patient blood samples, (B) (a–d) corresponding cells collected from the channel after separating the above patient blood samples, (C) separation of mixed cancer cell samples, and (D) independent separation of six cancer cell samples.

calculated the electric field strength applied to the membrane and the induced membrane voltage of cells (Djuzenova et al., 1994). The electric field and the induced membrane voltage were calculated to be 0.0008 kV/cm and $-6.0 \times 10^{-9}$ kV/cm, respectively. The loss of cell viability was usually shown with a field strength of >1 kV/cm in the previous works (Etienne et al., 2001; Colin, 2004). Therefore, the applied electric field does not cause cell death in the proposed system. The collected samples were subjected to multiple staining with fluorescein diacetate and propidium iodide to confirm cell viability. It was found that when the cells were subjected to the EMFC separation with the applied electric field and without the DM treatment, they were viable (Fig. S8). The toxicity was confirmed to be due to the anticancer drug. Hence, we are trying to find a suitable replacement for DM to be used as a recognition molecule with high affinity towards cancer cells and is electrochemically active.

## 4. Conclusions

In conclusion, the working principle of EMFC was evaluated using theoretical and practical evidences. We can demonstrate that the AC electric field application on the channel walls causes a strain on the cells in the channel fluid, resulting in an alternating movement of target species in the electric field direction that is perpendicular to the hydrodynamic flow. The resulting flow induces the oscillation of target species in the channel, bringing the same sized species together and enriching them. The device successfully identified different cancers by the means of isolation and detection of CTCs in human blood samples. The lipid-modified conductive polymer on the microfluidic channel walls showed a remarkable increase in the specific interaction with DM-decorated cancer cells and was able to separate and detect the CTCs in a short time period of 400 s. The frequency and amplitude of the applied electric field were optimized (10 kHz and 100 mV) such that two different cancer cells show maximum separation in the channel. The device was able to separate a single cell with 92.0 ± 0.5 % efficiency. 37 patient blood samples from different origins were separated and detected with the detection rate of 90.9%. Blind testing of the patient samples proved the reliability of the method to separate CTCs. In this preliminary study, different cancers were successfully discriminated in the patient samples using the proposed method. Hence, this method can be used in the development of cancer detection devices at an early stage.

## Declaration of competing interest

The authors declare that they have no known competing financial interests or personal relationships that could have appeared to influence the work reported in this paper.

## Acknowledgements

This work was supported by the National Research Foundation of Korea (NRF) grant funded by the Korea government (MSIP) (No. 2019R1A2C1002531).

## Appendix A. Supplementary data

Supplementary data to this article can be found online at https://doi.org/10.1016/j.bios.2019.111746.

## References

Adams, A.A., Okagbare, P.I., Feng, J., Hupert, M.L., Patterson, D., Gottert, J., McCarley, R.L., Nikitopoulos, D., Murphy, M.C., Soper, S.A., 2008. JACS 130, 8633–8641.
Ashworth, T.R., 1868. Melbourne Hospital Reports.
Bleilevens, C., Lolsberg, J., Cinar, A., Knoben, M., Grottke, O., Rossaint, R., Wessling, M., 2018. Sci. Rep. 8, 8031, 1-9.
Chandra, P., Noh, H.B., Shim, Y.B., 2013. Chem. Commun. 49, 1900–1902.
Colin, S., 2004. Microfluidique. Hermes Science, p. 54.
Desitter, I., Guerrouahen, B.S., Benali-Furet, N., Wechsler, J., Janne, P.A., Kuang, Y., Yanagita, M., Wang, L., Berkowitz, J.A., Distel, R.A., Cayre, Y.E., 2011. Anticancer Res. 31, 427–442.
Djuzenova, C.S., Sukhrukov, V.L., Klock, G., Arnold, W.M., Zimmermann, U., 1994. Cytometry 15, 35–45.
Etienne, G., Hulin, J.P., Petit, L., Mitescu, C., 2001. Physical Hydrodynamics. Oxford University Press.
Etzioni, R., Urban, N., Ramsey, S., McIntosh, M., Schwartz, S., Reid, B., Radich, J., Anderson, G., Hartwell, L., 2003. Nat. Rev. 3, 1–10.
Eunice, L.M., Manuel, M.M., 2013. In: Gregory, S.M. (Ed.), Advanves in Clinical Chemistry, vol. 61. Elsevier, pp. 175–224.
Guo, J., Liu, X., Kang, K., Ai, Ae, Wang, Z., Kang, Y., 2015. J. Light. Technol. 33 (16), 3433–3438.
Guo, J., Ma, X., Menon, N.V., Li, C.M., Zhao, Y., Kang, Y., 2015. IEEE J. Sel. Top. Quantum Electron. 21 (4), 7100107.
Gurudatt, N.G., Naveen, M.H., Ban, C., Shim, Y.B., 2016. Biosens. Bioelectron. 86, 33–40.
Jiang, Z., Le, N.D.B., Gupta, A., Rotello, V.M., 2015. Chem. Soc. Rev. 44, 4264–4274.
Kahn, H.J., Presta, A., Yang, L.Y., Blondal, J., Trudeau, M., Lickley, L., Holloway, C., McCready, D.R., Maclean, D., Marks, A., 2004. Breast Canc. Res. Treat. 86, 237–247.
Karabacak, N.M., Spuhler, P.S., Fachin, F., Lim, E.J., Pai, V., Ozkumur, E., Martel, J.M., Kojic, N., Smith, K., Chen, P., Yang, J., Hwang, H., Morgan, B., Trautwein, J., Barber, T.A., Stott, S.L., Maheshwaran, S., Kapur, R., Haber, D.A., Toner, M., 2014. Nat. Protoc. 9, 694–710.
Krivacic, R.T., Ladanyi, A., Curry, D.N., Kuhn, P., Bergsrud, D.E., Kepros, J.F., Barbera, T., Ho, M.Y., Chen, L.B., Lerner, R.A., Bruce, R.H., 2004. Proc. Natl. Acad. Sci. 101, 10501–10504.
Kwon, N.H., Rahman, M.A., Won, M.S., Shim, Y.B., 2006. Anal. Chem. 78, 52–60.
Lenshof, A., Laurell, T., 2009. Chem. Soc. Rev. 39, 1203–1217.
Li, P., Mao, Z., Peng, Z., Zhou, L., Chen, Y., Huang, P.H., Truica, C.I., Drabick, J.J., El-Deiry, W.S., Dao, M., Suresh, S., Huang, T.J., 2015. Proc. Natl. Acad. Sci. 112, 4970–4975.
Mehlen, P., Puisieux, A., 2006. Nat. Rev. 6, 449–458.
Moon, H.S., Kwon, K.S., Kim, I., Han, H., Sohn, J., Lee, S., Jung, H.I., 2011. Lab Chip 11, 1118–1125.
Nagrath, S., Sequist, L.V., Maheshwaran, S., Bell, D.W., Irimia, D., Ulkus, L., Smith, M.R., Kwak, E.L., Digumarthy, S., Muzikansky, A., Ryan, P., Balis, U.J., Tompkins, R.G., Haber, D.A., Toner, M., 2007. Nat. Lett. 450, 1235–1239.
Noh, H.B., Chandra, P., Kim, Y.J., Shim, Y.B., 2012. Anal. Chem. 84, 9738–9744.
Phillips, J.A., Xu, Y., Xia, Z., Fan, H.Z., Tan, W., 2009. Anal. Chem. 81, 1033–1039.
Rahman, M.A., Won, M.S., Shim, Y.B., 2003. Anal. Chem. 75, 1123–1129.
Rolle, A., Gunzel, R., Pachmann, U., Willen, B., Hoffken, K., Pachmann, K., 2005. World J. Surg. Oncol. 3 (18), 1–9.
Sanders, E.J., 1989. Cell Surface Embryogenesis Carcinogenesis: Common Mechanisms. Telford Press, Caldwell, pp. 121–161.
Tang, W., Jiang, D., Li, Z., Zhu, L., Shi, J., Yang, J., Xiang, N., 2019. Electrophoresis 40, 930–954.
Varki, A., Kannagi, R., Toole, B.P., 2009. Essentials of glycobiology. In: Chapter 44-Glycosylation Changes in Cancer (A. Varki, R. D. Cummings, J. D. Esko), second ed. Cold Spring Harbour Laboratory Press, New York.
Yeom, E., Kang, Y.J., Lee, S.J., 2014. Biomicrofluidics 8, 034110.
Zhang, Z., Nagrath, S., 2013. Biomed. Microdevices 15, 595–609.
Zieglschmid, V., Hollmann, C., Bocher, O., 2005. Crit. Rev. Clin. Lab. Sci. 42, 155–196.